

Efficient Column Generation for Cell Detection and Segmentation

Chong Zhang^{a,*}, Shaofei Wang^b, Miguel A. Gonzalez-Ballester^{a,c}, Julian Yarkony^{d,*}

^a*SimBioSys, DTIC, Universitat Pompeu Fabra, Barcelona, Spain*

^b*A&E Technologies, Beijing, China*

^c*ICREA, Spain*

^d*Experian Data Lab, USA*

Abstract

We study the problem of instance segmentation in biological images with crowded and compact cells. We formulate this task as an integer program where variables correspond to cells and constraints enforce that cells do not overlap. To solve this integer program, we propose a column generation formulation where the pricing program is solved via exact optimization of very small scale integer programs. Column generation is tightened using odd set inequalities which fit elegantly into pricing problem optimization. Our column generation approach achieves fast stable anytime inference for our instance segmentation problems. We demonstrate on three distinct light microscopy datasets, with several hundred cells each, that our proposed algorithm rapidly achieves or exceeds state of the art accuracy.

Keywords: Combinatorial optimization, Column generation, Integer programming, Large scale optimization, Linear programming

1. Introduction

Cell detection and instance segmentation are fundamental tasks for the study of bioimages (Meijering, 2012) in the era of big data. Detection corresponds

*Corresponding author

Email addresses: chong.zhang@upf.edu (Chong Zhang), julian.e.yarkony@gmail.com (Julian Yarkony)

to the problem of identifying individual cells and instance segmentation corresponds to the problem of determining the pixels corresponding to each of the cells. Cells are often in close proximity and/or occlude each other. Traditionally bioimages were manually analyzed, however recent advances in microscope techniques, automation, long-term high-throughput imaging, etc, result in vast amounts of data from biological experiments, making manual analysis, and even many computer aided methods with hand-tuned parameters, infeasible (Meijering et al., 2016; Hilsenbeck et al., 2017). The large diversity of cell lines and microscopy imaging techniques require the development of algorithms for these tasks to perform robustly and well across data sets.

In this paper we introduce a novel approach for instance segmentation specialized to bioimage analysis designed to rapidly produce high quality results with little human intervention. The technique described in this paper is applicable to images that have crowded and compact cell regions acquired from different modalities and cell shapes, as long as they produce intensity changes at cell boundaries. Such patterns result from several microscopy imaging techniques, such as trans-illumination (e.g. bright field, dark field, phase contrast) and fluorescence (e.g. through membrane or cytoplasmic staining) images. Thus it is specifically suitable for images from which cells are almost transparent.

We formulate instance segmentation as the problem of selecting a set of visually meaningful cells under the hard constraint that no two cells overlap (share a common pixel). This problem corresponds to the classic integer linear programming (ILP) formulation of the set packing problem (Karp, 1972) where sets correspond to cells and elements correspond to pixels. The number of possible cells is very large and can not be easily enumerated. We employ a column generation approach (Barnhart et al., 1996) for solving the combinatorial problem where the pricing problem is solved via exact optimization of very small scale integer programs (IPs). Inference is made tractable by relying on the assumption that cells are small and compact. When needed we tighten the linear programming (LP) relaxation using odd set inequalities (Heismann and Borndörfer, 2014). The use of odd set inequalities in our context does

not destroy the structure of the pricing problem so branch and price (Barnhart et al., 1996) is not needed.

For the purpose of dimensionality reduction we employ the common technique of aggregating pixels into superpixels. Superpixels (Levinshtein et al., 2009; Achanta et al., 2012) are the output of a dimensionality reduction technique that groups pixels in a close proximity with similar visual characteristics and is commonly used as a preprocessing for image segmentation (Arbelaez et al., 2011). Superpixels provide a gross over-segmentation of the image meaning that they capture many boundaries not in the ground truth but miss very few boundaries that are part of the ground truth. Hence we apply our set packing formulation on the superpixels meaning that each set corresponds to a subset of the superpixels and each element is a superpixel.

Our contributions consist of the following:

- Novel formulation of cell instance segmentation amenable to the tools and methodology of the operations research community
- Structuring our formulation to admit tightening the corresponding LP relaxation outside of branch/price methods
- Achieve benchmark level results on real microscopy datasets

We structure this document as follows. In Section 2 we consider the related work in the fields of bioimage analysis and operations research. Next in Section 3 we introduce our set packing formulation of instance segmentation and our column generation formulation with its corresponding pricing problem. Next in Sections 4 and 5 we consider the production of anytime integral solutions and lower bounds respectively. In Section 6 we demonstrate the applicability of our approach to real bioimage data sets. Finally we conclude and consider extensions in Section 7.

2. Related Work

2.1. Optimization in computer vision and bioimage analysis

Our work should be considered in the context of methods that are based on cell boundary information and clustering of super-pixels. Relevant methodologies include contour profile pattern (Kvarnström et al., 2008; Mayer et al., 2013; Dimopoulos et al., 2014), constrained label cost model (Zhang et al., 2014a), correlation clustering (Zhang et al., 2014b; Yarkony et al., 2015), structured learning (Arteta et al., 2012; Liu et al., 2014; Funke et al., 2015), and deep learning (Ronneberger et al., 2015), etc. A comprehensive review can be found in (Xing and Yang, 2016). Here we discuss the most relevant work.

The method of (Zhang et al., 2014b) frames instance segmentation as correlation clustering on a planar or nearly planar graph and relies heavily on the planarity of their clustering problem’s structure in order to achieve efficient inference. Our work differs from (Zhang et al., 2014b) primarily from the perspective of optimization. Notably, our model is not bound by planarity restrictions and instead relies on the assumption that cells are typically small and compact. Therefore, our model is also applicable to 3D segmentation.

In (Zhang et al., 2015) the authors use depth to transform instance segmentation into a labeling problem and thus break the difficult symmetries found in instance segmentation. They formulate the optimization as an ILP and solve it using greedy network flow methods (Boykov et al., 2001), notably the Quadratic Pseudo-Boolean optimization (QPBO) (Boros and Hammer, 2002; Rother et al., 2007). The approach in (Zhang et al., 2015) also requires prior knowledge of the number of labels present in the image, which is not realistic for images crowded with hundreds or thousands of cells. In contrast our proposed ILP framework does not require knowledge of the number of objects in the image.

Our inference approach is inspired by (Wang et al., 2017a) which tackles multi-object tracking using column generation where the corresponding pricing problem is solved using dynamic programming. This echoes the much earlier operations research work in diverse areas such as vehicle routing (Ropke and

Cordeau, 2009), and cutting stock (Gilmore and Gomory, 1961) which use dynamic programming for pricing. In contrast our pricing problem optimization is solved by many small ILPs, which can be run in parallel which echoes the work in the operations research community of (Barahona and Jensen, 1998).

2.2. Column generation in operations research

Column generation (Gilmore and Gomory, 1961; Desaulniers et al., 2006; Barnhart et al., 1996) is a popular approach for solving ILPs in which compact formulations result in loose LP relaxations where the fractional solution tends to be uninformative. Here uninformative means that the fractional solution can not easily be rounded to a low cost integer solution. Column generation replaces the LP with a new LP over a much larger space of variables which corresponds to a tighter LP relaxation of the ILP (Geoffrion, 2010; Armacost et al., 2002). The new LP retains the property from the original LP that it has a finite number of constraints.

To solve the new LP, the dual of the new LP is considered which has a finite number of variables and a huge number of constraints. Optimization considers only a limited subset of the primal variables, which is initialized as empty, or set heuristically. Optimization alternates between solving the LP relaxation over the limited subset of the primal variables (called the master problem) and identifying variables that correspond to violated dual constraints (which is called pricing). Pricing often corresponds to combinatorial optimization which is often an elegant dynamic program which has the powerful feature that many primal variables (violated dual constraints) are generated at once. Approaches with dynamic programming based pricing include (but are not limited to) the diverse fields of cutting stock (Gilmore and Gomory, 1961, 1965), routing crews (Lavoie et al., 1988; Vance et al., 1997), and routing vehicles (Ropke and Cordeau, 2009),

Column generation formulations can be tightened using branch-price methods (Barnhart et al., 2000, 1996; Vance, 1998) which is a variant of branch and bound (Land and Doig, 1960) that is structured as to not disrupt the structure of the pricing problem.

Term	Form	Index	Meaning
\mathcal{D}	set	d	set of super-pixels
\mathcal{Q}	set	q	set of cells
Q	$\{0, 1\}^{ \mathcal{D} \times \mathcal{Q} }$	d, q	$Q_{dq} = 1$ indicates that d in cell q
Γ	$\mathbb{R}^{ \mathcal{Q} }$	q	Γ_q is the cost of cell q
\mathcal{C}	set	c	set of triples
γ	$\{0, 1\}^{ \mathcal{Q} }$	q	$\gamma_q = 1$ indicates that cell q is selected.
θ	$\mathbb{R}^{ \mathcal{D} }$	d	θ_d is the cost of including d in a cell
ω	\mathbb{R}	none	ω is the cost of instancing a cell
ϕ	$\mathbb{R}^{ \mathcal{D} \times \mathcal{D} }$	d_1, d_2	$\phi_{d_1 d_2}$ is the cost of including d_1, d_2 in the same cell
V	$\mathbb{R}_{0+}^{ \mathcal{D} }$	d	V_d is the volume of super-pixel d
S	$\mathbb{R}_{0+}^{ \mathcal{D} \times \mathcal{D} }$	d_1, d_2	$S_{d_1 d_2}$ is the distance between the centers of super-pixels d_1, d_2
m_V	\mathbb{R}_+	none	maximum volume of a cell
m_R	\mathbb{R}_+	none	maximum radius of a cell
$\hat{\mathcal{Q}}$	set	q	set of cells generated during column generation
$\hat{\mathcal{C}}$	set	c	set of triples generated during column generation
$\dot{\mathcal{Q}}$	set	q	set of cells generated during a given iteration of column generation
$\dot{\mathcal{C}}$	set	c	set of triples generated during a given iteration of column generation
λ	$\mathbb{R}_{0+}^{ \mathcal{D} }$	d	Lagrange multipliers corresponding to super-pixels
κ	$\mathbb{R}_{0+}^{ \mathcal{C} }$	c	Lagrange multipliers corresponding to triples
x	$\{0, 1\}^{ \mathcal{D} }$	d	$x_d = 1$ indicates that super-pixel d is included in the column being generated

Table 1: Summary of Notation

Column generation has had few applications in computer vision until recently but has included diverse variants of correlation clustering (Yarkony and Fowlkes, 2015; Yarkony et al., 2012; Yarkony, 2015) with applications to image partitioning, multi-object tracking (Wang et al., 2017a), and multi-human pose estimation (Wang et al., 2017b). Column generation in (Yarkony and Fowlkes, 2015; Yarkony et al., 2012; Yarkony, 2015) is notable in that the pricing problem is solved using the max cut on a planar graph (Shih et al., 1990; Barahona, 1982, 1991; Barahona and Mahjoub., 1986) which is known to be polynomial time solvable via a reduction to perfect matching (Fisher, 1966).

3. Problem formulation

We now discuss our approach in detail. Given an image we start with computing a set of super-pixels (generally named super-voxels in 3D), which provides

an over-segmentation of cells. These super-pixels are then clustered into “perceptually meaningful” regions by constructing an optimization problem that either groups the super-pixels into small coherent cells or labels them as background. The solution to this optimization problem corresponds to the globally optimal selection of cells according to our model, which we formulate/solve as an ILP. We consider our model below and summarize the corresponding notation in Table 1.

Definitions. Let \mathcal{D} be the set of super-pixels in an image, \mathcal{Q} be the set of all possible cells, and $G \in \{0, 1\}^{|\mathcal{D}| \times |\mathcal{Q}|}$ be the super-pixel/cell incidence matrix where $G_{dq}=1$ if and only if super-pixel d is part of the cell q . We use $S \in \mathbb{R}_{0+}^{|\mathcal{D}| \times |\mathcal{D}|}$ to describe the Euclidean distance between super-pixels; where $S_{d_1 d_2}$ indicates the distance between the centers of the super-pixel pair d_1 and d_2 . We use $V \in \mathbb{R}_+^{|\mathcal{D}|}$ to describe the area of super-pixels, with V_d being the area of super-pixel d . The indicator vector $\gamma \in \{0, 1\}^{|\mathcal{Q}|}$ gives a feasible segmentation solution, where $\gamma_q=1$ indicates that cell q is included in the solution and $\gamma_q=0$ otherwise. A collection of cells specified by γ is a valid solution if and only if each super-pixel is associated with at most one active cell.

We use $\Gamma \in \mathbb{R}^{|\mathcal{Q}|}$ to define a cost vector, where Γ_q is the cost associated with including cell q in the segmentation. Here we model such a cost with terms $\theta \in \mathbb{R}^{|\mathcal{D}|}$ and $\phi \in \mathbb{R}^{|\mathcal{D}| \times |\mathcal{D}|}$ which are indexed by d and d_1, d_2 respectively. We use θ_d to denote the cost for including d in a cell and $\phi_{d_1 d_2}$ to denote the cost for including d_1 and d_2 in the same cell. We use $\omega \in \mathbb{R}$ to denote the cost of instancing a cell. We now define Γ_q in terms of θ , ϕ and ω .

$$\Gamma_q = \omega + \sum_{d \in \mathcal{D}} \theta_d G_{dq} + \sum_{d_1, d_2 \in \mathcal{D}} \phi_{d_1 d_2} G_{d_1 q} G_{d_2 q}, \quad (1)$$

Constraints. For most biological problems, it is valid to model cells of a given type as having a maximum radius m_R and a maximum area (volume if in 3D) m_V . Clearly, m_V and m_R are model defined parameters that vary from one application to another, but they are also often known a-priori. The radius

Term	Effect of Positive Offset
θ	Decrease total volume of cells
ϕ	Fewer pairs of super-pixels in a common cell
ω	Decrease number of cells detected
m_V	Increase maximum volume of cells
m_R	Increase maximum radius of cells

Table 2: Summary of effect of offsetting values by positive offset

constraint can be written as follows:

$$\exists[d_*; G_{d_*q} = 1] \quad \text{s.t.} \quad 0 = \sum_{d_2 \in \mathcal{D}} G_{d_2q} [S_{d_*, d_2} > m_R] \quad \forall q \in \mathcal{Q}. \quad (2)$$

For any given $q \in \mathcal{Q}$, any argument $d_* \in \mathcal{D}$ satisfying Eq 2 is called an anchor of q . Similarly, we write the area constraint as follows.

$$m_V \geq \sum_{d \in \mathcal{D}} G_{dq} V_d \quad \forall q \in \mathcal{Q}. \quad (3)$$

ILP formulation. Given the above variable definitions, we frame instance segmentation as an ILP that minimizes the total cost of the selected cells:

$$\min_{\substack{\gamma_q \in \{0,1\} \forall q \in \mathcal{Q} \\ \sum_{q \in \mathcal{Q}} G_{dq} \gamma_q \leq 1 \quad \forall d \in \mathcal{D}}} \sum_{q \in \mathcal{Q}} \Gamma_q \gamma_q = \min_{\substack{\gamma \in \{0,1\}^{|\mathcal{Q}|} \\ G\gamma \leq 1}} \Gamma^\top \gamma \quad (4)$$

The effect of our modeling parameters is summarized in Table 2.

Primal and Dual formulation. The LP relaxation of Eq 4 only contains constraints for cells that share a common super-pixel. This generally results in a tight relaxation, although not always. We tighten the relaxation using odd set inequalities (Heismann and Borndörfer, 2014). Specifically we use odd set inequalities of size three, (called triples), as similarly imposed in (Wang et al., 2017a).

Triples are defined as follows: for any set of three unique super-pixels (called a triple) the number of selected cells of \mathcal{Q} that include two or more of super-pixels in $\{d_1, d_2, d_3\}$ can be no larger than one, i.e.

$$\sum_{q \in \mathcal{Q}} [G_{d_1q} + G_{d_2q} + G_{d_3q} \geq 2] \gamma_q \leq 1. \quad (5)$$

We denote the set of triples as \mathcal{C} and describe it by a constraint matrix $C \in \{0, 1\}^{|\mathcal{C}| \times |\mathcal{Q}|}$, where $C_{cq} = 1$ if and only if cell q contains two or more members of set c . The constraint matrix has a row for each triple: $C_{cq} = [\sum_{d \in c} G_{dq} \geq 2], \forall c \in \mathcal{C}, q \in \mathcal{Q}$. The primal and dual LP relaxations of instance segmentation with constraints on inequalities corresponding to triples are written below. The dual is expressed using Lagrange multipliers $\lambda \in \mathbb{R}_{0+}^{|\mathcal{D}|}$ and $\kappa \in \mathbb{R}_{0+}^{|\mathcal{C}|}$.

$$\min_{\substack{\gamma \geq 0 \\ Q\gamma \leq 1 \\ C\gamma \leq 1}} \Gamma^\top \gamma = \max_{\substack{\lambda \geq 0 \\ \kappa \geq 0 \\ \Gamma + Q^\top \lambda + C^\top \kappa \geq 0}} 1^\top \lambda + 1^\top \kappa. \quad (6)$$

3.1. Algorithm

Since \mathcal{Q}, \mathcal{C} are intractably large, we use cutting plane method in the primal and dual to build a sufficient subsets of \mathcal{Q}, \mathcal{C} .

We denote the nascent subsets of \mathcal{Q}, \mathcal{C} as $\hat{\mathcal{Q}}, \hat{\mathcal{C}}$ respectively. In Alg 1 we write column generation algorithm. We define the cutting plane/column generation in Sections 3.2 and 3.3 respectively and display optimization in Fig 1. We use $\hat{\mathcal{Q}}, \hat{\mathcal{C}}$ to refer to the columns and rows generated during a given iteration of our algorithm.

Algorithm 1 Dual Optimization

```

 $\hat{\mathcal{Q}} \leftarrow \{\}$ 
 $\hat{\mathcal{C}} \leftarrow \{\}$ 
repeat
   $\dot{\mathcal{Q}} \leftarrow \{\}$ 
   $\dot{\mathcal{C}} \leftarrow \{\}$ 
   $[\lambda, \kappa, \gamma] \leftarrow \text{Solve Primal and Dual of Eq 6 over } \hat{\mathcal{Q}}, \hat{\mathcal{C}}$ 
  for  $d_* \in \mathcal{D}$  do
     $q_* \leftarrow \arg \min_{\substack{q \in \mathcal{Q} \\ Q_{d_* q} = 1 \\ 0 = \sum_{d_2 \in \mathcal{D}} G_{d_2 q} [S_{d_*, d_2} > m_R]}} \Gamma_q + \sum_{d \in \mathcal{D}} Q_{dq} \lambda_d + \sum_{c \in \mathcal{C}} \kappa_c [2 \leq \sum_{d \in \mathcal{C}} Q_{dq}]$ 
    if  $\Gamma_{q_*} + \sum_{d \in \mathcal{D}} Q_{dq_*} \lambda_d + \sum_{c \in \mathcal{C}} \kappa_c [2 \leq \sum_{d \in \mathcal{C}} Q_{dq}] < 0$  then
       $\dot{\mathcal{Q}} \leftarrow [\dot{\mathcal{Q}} \cup q_*]$ 
    end if
  end for
   $c_* \leftarrow \max_{c \in \mathcal{C}} \sum_{q \in \mathcal{Q}} C_{cq} \gamma_q$ 
  if  $\sum_{q \in \mathcal{Q}} C_{cq} \gamma_q > 1$  then
     $\dot{\mathcal{C}} \leftarrow c_*$ 
  end if
   $\hat{\mathcal{Q}} \leftarrow [\hat{\mathcal{Q}}, \dot{\mathcal{Q}}]$ 
   $\hat{\mathcal{C}} \leftarrow [\hat{\mathcal{C}}, \dot{\mathcal{C}}]$ 
until  $\dot{\mathcal{Q}} = []$  and  $\dot{\mathcal{C}} = []$ 

```

3.2. Row generation

Finding the most violated row consists of the following optimization.

$$\max_{c \in \mathcal{C}} \sum_{q \in \mathcal{Q}} C_{cq} \gamma_q \quad (7)$$

Enumerating \mathcal{C} is unnecessary and we generate its rows as needed by considering only $c = \{d_{c_1} d_{c_2} d_{c_3}\}$ such that for each of pair d_{c_i}, d_{c_j} there exists an index q such that $\gamma_q > 0$ and $Q_{d_i q} = Q_{d_j q} = 1$. Generating rows is done only when no (significantly) violated columns exist. Triples are only added to $\hat{\mathcal{C}}$ if the

corresponding constraint is violated. We can add one or more than one per iteration depending on a schedule chosen.

3.3. Generating columns

Violated constraints in the dual correspond to primal variables (cells) that may improve the primal objective. To identify such primal variables we compute for each $d_* \in \mathcal{D}$ the most violated dual constraint corresponding to a cell such that d_* is an anchor of that cell. The corresponding cell is described using indicator vector $x \in \{0, 1\}^{|\mathcal{D}|}$, where the corresponding column is defined as $Q_{dq} \leftarrow x_d, \forall d \in \mathcal{D}$. We write the pricing problem as an IP below.

$$\begin{aligned}
& \min_{x \in \{0, 1\}^{|\mathcal{Q}|}} \sum_{d \in \mathcal{D}} (\theta_d + \lambda_d) x_d + \sum_{d_1, d_2 \in \mathcal{D}} \phi_{d_1 d_2} x_{d_1} x_{d_2} + \sum_{c \in \mathcal{C}} \kappa_c ([2 \leq \sum_{d \in c} x_d]) \\
& \text{s.t. } x_{d_*} = 1 \\
& x_d = 0 \quad \forall d \in \mathcal{D} \quad \text{s.t. } S_{d, d_*} > m_R \\
& \sum_{d \in \mathcal{D}} V_d x_d \leq m_V
\end{aligned} \tag{8}$$

For our data sets of images crowded with several hundreds of cells, the maximum radius of a cell is relatively small and the number of super-pixels within the radius of a given super-pixel is of the order of tens and often around ten. Therefore, solving Eq 8 is efficient and can be done in parallel for each $d_* \in \mathcal{D}$. We tackle this by converting Eq 8 to an ILP and then solving it with an off-the-shelf ILP solver.

4. Anytime Integral Solutions

We now consider the anytime production of integral solutions in the master problem. While set packing NP hard in general, in practice the LP relaxations are integral at termination and generally integral after each step of optimization. For cases where the LP is loose, we find that solving the ILP given the primal variables generated takes little additional time beyond solving the LP. However we can use rounding procedures (Wang et al., 2017a) when difficult

Algorithm 2 Upper Bound Rounding

while $\exists q \in \mathcal{Q}$ s.t. $\gamma_q \notin \{0, 1\}$ **do**
 $q^* \leftarrow \arg \min_{\substack{q \in \mathcal{Q} \\ 1 > \gamma_q > 0}} \Gamma_q \gamma_q - \sum_{\hat{q} \in \mathcal{Q}_{\perp q}} \Gamma_{\hat{q}} \gamma_{\hat{q}}$
 $\gamma_{\hat{q}} \leftarrow 0 \quad \forall \hat{q} \in \mathcal{Q}_{\perp q^*}$
 $\gamma_{q^*} \leftarrow 1$
end while
RETURN γ

ILPs occur. Specifically, we tackle the rounding of a fractional γ with a greedy iterative approach. At each iteration, it selects the cell q with non-binary γ_q that minimizes $\Gamma_q \gamma_q$ discounted by the fractional cost of any cells that share a super-pixel with q ; hence can no longer be added to the segmentation if q is already added. We write the rounding procedure in Alg 2 using the notation $\mathcal{Q}_{\perp q}$ to indicate the set of cells in \mathcal{Q} that intersect cell q (excluding q itself).

5. Lower bounds

We now consider the production of anytime lower bounds on the optimal integral solution. We first write the ILP for cell instance segmentation and then introduce Lagrange multipliers.

$$\min_{\substack{\gamma \in \{0,1\}^{|\mathcal{Q}|} \\ Q\gamma \leq 1 \\ C\gamma \leq 1}} \Gamma^\top \gamma = \min_{\substack{\gamma \in \{0,1\}^{|\mathcal{Q}|} \\ Q\gamma \leq 1}} \max_{\substack{\lambda \geq 0 \\ \kappa \geq 0}} \Gamma^\top \gamma + (-\lambda^\top 1 + \lambda^\top Q\gamma) + (-\kappa^\top 1 + \kappa^\top C\gamma) \quad (9)$$

We now relax the constraint in Eq 9 that the dual variables are optimal producing the following lower bound.

$$\begin{aligned} \text{Eq 9} &\geq \min_{\substack{\gamma \in \{0,1\}^{|\mathcal{Q}|} \\ Q\gamma \leq 1}} \Gamma^\top \gamma + (-\lambda^\top 1 + \lambda^\top Q\gamma) - (\kappa^\top 1 + \kappa^\top C\gamma) \\ &= -\kappa^\top 1 - \lambda^\top 1 + \min_{\substack{\gamma \in \{0,1\}^{|\mathcal{Q}|} \\ Q\gamma \leq 1}} (\Gamma + Q^\top \lambda + C^\top \kappa)^\top \gamma \end{aligned} \quad (10)$$

Recall that every cell is associated with at least one anchor. We denote the set of anchors associated with a given cell q as \mathcal{N}_q . We use $Q_{:,q}$, $C_{:,q}$ to refer to the

column q of the matrices Q, C respectively. Given any fixed $\gamma \in \{0, 1\}^{|\mathcal{Q}|}$ such that $Q\gamma \leq 1$ observe the following.

$$(\Gamma + Q^\top \lambda + C^\top \kappa)^\top \gamma \geq \sum_{d \in \mathcal{D}} \min[0, \min_{\substack{q \in \mathcal{Q} \\ d \in \mathcal{N}_q}} \gamma_q (\Gamma_q + Q_{:,q}^\top \lambda + C_{:,q}^\top \kappa)] \quad (11)$$

We now use Eq 11 to produce following lower bound on Eq 10.

$$\text{Eq 10} \geq -\kappa^\top 1 - \lambda^\top 1 + \min_{\substack{\gamma \in \{0,1\}^{|\mathcal{Q}|} \\ Q\gamma \leq 1}} \sum_{d \in \mathcal{D}} \min[0, \min_{\substack{q \in \mathcal{Q} \\ d \in \mathcal{N}_q}} \gamma_q (\Gamma_q + Q_{:,q}^\top \lambda + C_{:,q}^\top \kappa)] \quad (12)$$

We now relax the constraint in Eq 12 that $Q\gamma \leq 1$ producing the following lower bound.

$$\begin{aligned} \text{Eq 12} &\geq -\kappa^\top 1 - \lambda^\top 1 + \min_{\gamma \in \{0,1\}^{|\mathcal{Q}|}} \sum_{d \in \mathcal{D}} \min[0, \min_{\substack{q \in \mathcal{Q} \\ d \in \mathcal{N}_q}} \gamma_q (\Gamma_q + Q_{:,q}^\top \lambda + C_{:,q}^\top \kappa)] \\ &= -\kappa^\top 1 - \lambda^\top 1 + \sum_{d \in \mathcal{D}} \min[0, \min_{\substack{q \in \mathcal{Q} \\ d \in \mathcal{N}_q}} (\Gamma_q + Q_{:,q}^\top \lambda + C_{:,q}^\top \kappa)] \end{aligned} \quad (13)$$

Observe that the term $\min_{\substack{q \in \mathcal{Q} \\ d \in \mathcal{N}_q}} (\Gamma_q + Q_{:,q}^\top \lambda + C_{:,q}^\top \kappa)$ is identical to the optimization computed at every stage of column generation.

6. Results

The technique described in this paper is applicable to images crowded with cells which are mainly discernible by boundary cues. Such images can be acquired from different modalities and cell types. Here we evaluate our algorithm on three datasets. Challenges of these datasets include: densely packed and touching cells, out-of-focus artifacts, variations on shape and size, changing boundaries even on the same cell, as well as other structures showing similar boundaries.

6.1. Experiment settings

To ensure detecting cell boundaries with varying patterns, a trainable classifier seems to be the right choice. For each dataset, we choose to train a Random Forest (RF) classifier from the open source software, ilastik (Sommer et al.,

2011), to discriminate: (1) boundaries of in-focus cells; (2) in-focus cells; (3) out-of-focus cells; and (4) background. The posterior probabilities for class (1) is used as the pairwise potentials. For training, we used $< 1\%$ pixels per dataset with generic features e.g. Gaussian, Laplacian, Structured tensor. Subsequent steps use the posterior probabilities to calculate parameters and require no more training. The prediction from the class boundaries of in-focus cells is also used to generate super-pixels. And those for classes (3) and (4) are combined and inverted to create a foreground prediction. Here foreground corresponds to the superpixels that are part of cells which are background otherwise. For each super-pixel, the proportion of its foreground part defines the unary potential θ which we then offset by a constant fixed for each dataset. A summary about the parameters used in our experiments are shown in Table 3.

6.2. Evaluation

A visualization of the results can be seen in Fig 2. Quantitatively, we compare the performance of our algorithm with those reported in the state-of-the-art methods (Arteta et al., 2012, 2016; Funke et al., 2015; Hilsenbeck et al., 2017; Dimopoulos et al., 2014; Ronneberger et al., 2015; Zhang et al., 2014b), in terms of detection (precision, recall and F-score) and segmentation (Dice coefficient and Jaccard index). For detection, we establish possible matches between found regions and ground truth (GT) regions based on overlap, and find a Hungarian matching using the centroid distance as minimizer. Unmatched GT regions are FN, unmatched segmentation regions are FP. Jaccard index is computed between the area of true positive (TP) detection regions R_{tpd} and the area of GT region R_{gt} : $(R_{tpd} \cap R_{gt}) / (R_{tpd} \cup R_{gt})$. They are summarized in Tables 4 and 5. In general, our method achieves or exceed state of the art performance. Additionally, our method requires very little training for the RF classifiers, as opposed to methods like (Arteta et al., 2012, 2016; Funke et al., 2015), which require fully labeled data for training. This is an advantage of relieving human annotations when several hundreds of cells need to be labeled per image. Also, our method can handle very well large variations of cell shape/size even in the

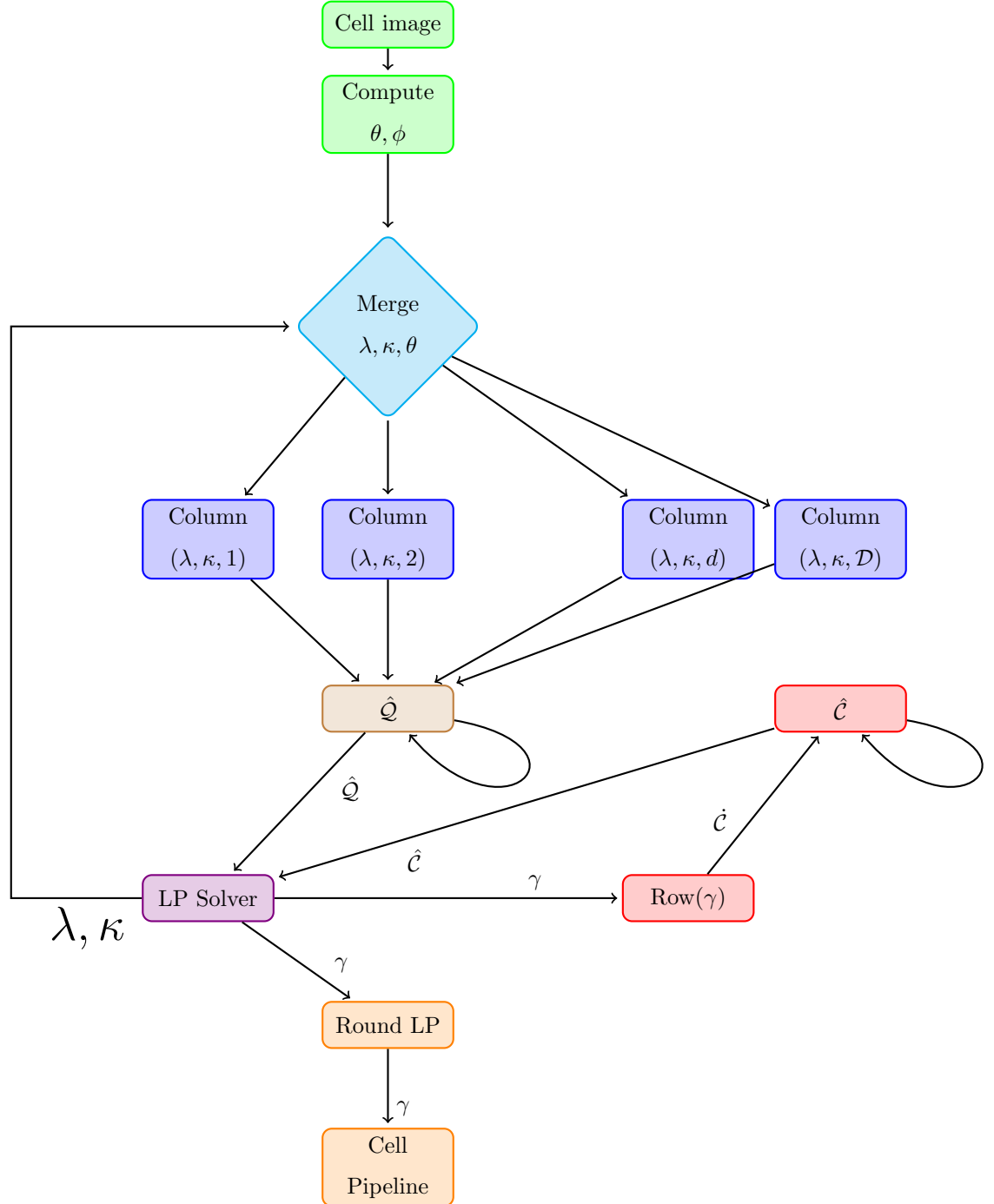


Figure 1: Overview of our system. We use colors to distinguish between the different parts of the system, which are defined as follows: user input (*green*), sub-problem solution (*blue*), triples (*red*), rounding the output of the LP solver (*orange*). We use $\text{Column}(\lambda, \kappa, d)$ to refer to generating the column where d is an anchor.

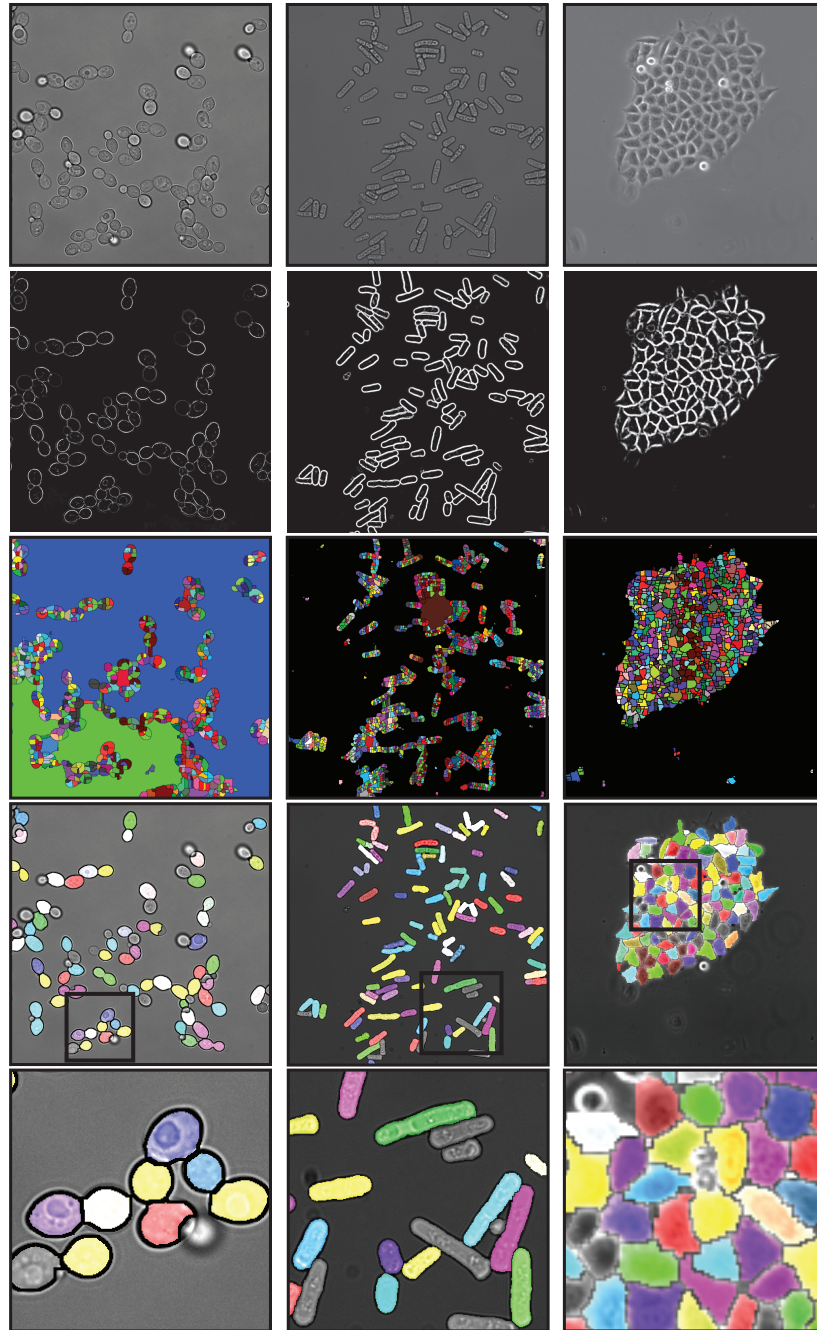


Figure 2: Example cell segmentation results of Datasets 1-3 (*left to right*). Rows are (*top to bottom*): original image, cell of interest boundary classifier prediction image, super-pixels, color map of segmentation, and enlarged views of the inset (*black square*)

Table 3: Summary of experimental datasets on the number of cells, cell radius, image size, the number of super-pixels and region adjacent graph (RAG) edges.

Dataset	# cells	avg. cell radius	image size	# super-pixels	# RAG edges
1 (Zhang et al., 2014a)	1768	30	1024×1024	1225 ± 242	3456 ± 701
2 (Peng et al., 2013)	2340	50	1024×1024	3727 ± 2450	10530 ± 7010
3 (Arteta et al., 2012)	1073	20	400×400	1081 ± 364	3035 ± 1038

Table 4: Evaluation and comparison of detection for Datasets 1-3 (Fig. 2) on precision (P), recall (R), F-score (F), dice coefficient (D) and Jaccard index (J) are reported for the proposed method, as well as those reported in the state-of-the-art methods. Here (Zhang et al., 2014b) uses the algorithms planar correlation clustering (PCC) and non-planar correlation clustering (NPCC).

	Dataset 1			Dataset 2			Dataset 3		
	P	R	F	P	R	F	P	R	F
(Arteta et al., 2012)	-	-	-	-	-	-	0.89	0.86	0.87
(Arteta et al., 2016)	-	-	-	-	-	-	0.99	0.96	0.97
(Funke et al., 2015)	0.93	0.89	0.91	0.99	0.90	0.94	0.95	0.98	0.97
(Hilsenbeck et al., 2017)	-	-	-	-	-	-	-	-	0.97
(Ronneberger et al., 2015)	-	-	-	-	-	-	-	-	0.97
PCC (Zhang et al., 2014b)	0.95	0.86	0.90	0.80	0.75	0.76	0.92	0.92	0.92
NPCC (Zhang et al., 2014b)	0.71	0.96	0.82	0.75	0.83	0.78	0.85	0.97	0.90
<i>Proposed</i>	0.99	0.97	0.98	1.00	0.94	0.97	1.00	0.97	0.99

Table 5: Evaluation and comparison of segmentation for Datasets 1-3 (Fig. 2) on dice coefficient (D) and Jaccard index (J) are reported for the proposed method, as well as those reported in the state-of-the-art methods. Here (Zhang et al., 2014b) uses the algorithms planar correlation clustering (PCC) and non-planar correlation clustering (NPCC).

	Dataset 1		Dataset 2		Dataset 3	
	D	J	D	J	D	J
(Funke et al., 2015)	0.90	0.82	0.90	0.83	0.84	0.73
(Hilsenbeck et al., 2017)	-	-	-	-	-	0.75
(Dimopoulos et al., 2014)	-	0.87	-	-	-	-
(Ronneberger et al., 2015)	-	-	-	-	-	0.74
PCC (Zhang et al., 2014b)	0.87	0.84	0.91	0.85	0.79	0.72
NPCC (Zhang et al., 2014b)	0.86	0.89	0.91	0.84	0.80	0.70
<i>Proposed</i>	0.91	0.90	0.90	0.83	0.82	0.71

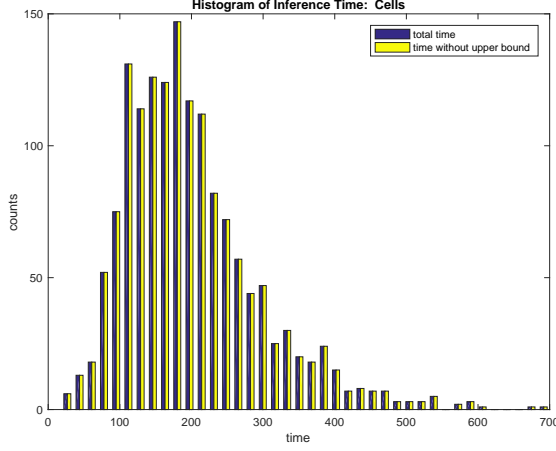


Figure 3: Histogram of inference time for Dataset 1.

same image, as shown in Fig 2 for Dataset 2.

6.3. Timing and bounds

We now consider the performance of our approach with regard to the gap between the upper and lower bounds produced by our algorithm. We normalize these gaps by dividing by the absolute value of the lower bound. For our three data set the proportion of problem instances that achieve normalized gaps under 0.1 are 99.28 %, 80 % and 100 %, on Datasets 1,2,3 respectively. The peak histogram of inference time are around 150, 500 and 100 seconds without parallelization. As an example, the histogram of inference time for Dataset 1 is shown in Fig 3. Our approach is approximately an order of magnitude faster than that of (Zhang et al., 2014b).

7. Conclusion

In this article we introduce a novel column generation strategy that efficiently optimizes an ILP formulation of instance segmentation through clustering super-pixels. We use our approach to detect and segment crowded clusters of cells in

distinct microscopy image datasets and achieves state of the art or near state of the art performance.

We now consider some extensions of our approach. The use of odd set inequalities may prove useful for traditional set cover formulations of vehicle routing problems. In this context for triples the corresponding inequality is defined as follows: *For any set of three unique depots the number of routes that pass through one or two or those depots plus two times the number of routes that pass through all three depots is no less than two.* Dynamic programming formulations for pricing can be adapted to include the corresponding Lagrange multipliers (Irnich and Desaulniers, 2005) (in either the elementary or non-elementary (Kallehauge et al., 2005) setting). The approach in (Wang et al., 2017a) can also be adapted which employs dynamic programming in a branch and bound context in the pricing problem (never the master problem).

Another extension considers multiple types of cells with a unique model for each cell type and its own pricing problem. Such types can include rotations, scalings, or other transformations of a common model which may be useful for cells that highly non-circular in shape.

In future work one should apply dual feasible inequalities (Ben Amor et al., 2006; Yarkony and Fowlkes, 2015). In this case one would create separate variable for each pair of cell, feasible anchor for that cell (where the anchor is called the the main anchor). Then the ILP would be framed as selecting a set of cells such that (1) no super-pixel is included more than once and (2) no main anchor is included in more than one cell. However the Lagrange multipliers for (1) can be bounded from above by the increase in cost corresponding to removing the super-pixel d from a cell. For a super-pixel d one trivial such bound is minus one times the sum of the non-positive cost terms involving d .

Acknowledgment

This work was partly supported by the Spanish Ministry of Economy and Competitiveness under the Maria de Maeztu Units of Excellence Programme (MDM-2015-0502).

References

- Achanta, R., Shaji, A., Smith, K., Lucchi, A., Fua, P., Ssstrunk, S., 2012. SLIC superpixels compared to state-of-the-art superpixel methods. *IEEE Transactions on Pattern Analysis and Machine Intelligence* 34, 2274–2282.
- Arbelaez, P., Maire, M., Fowlkes, C., Malik, J., 2011. Contour detection and hierarchical image segmentation. *IEEE Transactions on Pattern Analysis and Machine Intelligence* 33, 898–916.
- Armacost, A.P., Barnhart, C., Ware, K.A., 2002. Composite variable formulations for express shipment service network design. *Transportation Science* 36, 1–20.
- Arteta, C., Lempitsky, V., Noble, J., Zisserman, A., 2012. Learning to detect cells using non-overlapping extremal regions, in: *International Conference on Medical Image Computing and Computer Assisted Intervention (MICCAI)*. volume 7510 of *Lecture Notes in Computer Science*, pp. 348–356.
- Arteta, C., Lempitsky, V., Noble, J., Zisserman, A., 2016. Detecting overlapping instances in microscopy images using extremal region trees. *Medical Image Analysis* 27, 3–16.
- Barahona, F., 1982. On the computational complexity of ising spin glass models. *Journal of Physics A: Mathematical, Nuclear and General* 15, 3241–3253.
- Barahona, F., 1991. On cuts and matchings in planar graphs. *Mathematical Programming* 36, 53–68.
- Barahona, F., Jensen, D., 1998. Plant location with minimum inventory. *Mathematical Programming* 83, 101–111.
- Barahona, F., Mahjoub, A., 1986. On the cut polytope. *Mathematical Programming* 60, 157–173.

- Barnhart, C., Hane, C.A., Vance, P.H., 2000. Using branch-and-price-and-cut to solve origin-destination integer multicommodity flow problems. *Operations Research* 48, 318–326.
- Barnhart, C., Johnson, E.L., Nemhauser, G.L., Savelsbergh, M.W.P., Vance, P.H., 1996. Branch-and-price: Column generation for solving huge integer programs. *Operations Research* 46, 316–329.
- Ben Amor, H., Desrosiers, J., Valério de Carvalho, J.M., 2006. Dual-optimal inequalities for stabilized column generation. *Operations Research* 54, 454–463.
- Boros, E., Hammer, P., 2002. Pseudo-boolean optimization. *Discrete Applied Mathematics* 123, 155–225.
- Boykov, Y., Veksler, O., Zabih, R., 2001. Fast approximate energy minimization via graph cuts. *IEEE Transactions on Pattern Analysis and Machine Intelligence* 23, 1222–1239.
- Desaulniers, G., Desrosiers, J., Solomon, M.M., 2006. Column Generation. volume 5. Springer Science & Business Media.
- Dimopoulos, S., Mayer, C., Rudolf, F., Stelling, J., 2014. Accurate cell segmentation in microscopy images using membrane patterns. *Bioinformatics* 30, 2644–2651.
- Fisher, M.E., 1966. On the dimer solution of planar ising models. *Journal of Mathematical Physics* 7, 1776–1781.
- Funke, J., Hamprecht, F., Zhang, C., 2015. Learning to segment: Training hierarchical segmentation under a topological loss, in: International Conference on Medical Image Computing and Computer Assisted Intervention (MICCAI). volume 9351 of *Lecture Notes in Computer Science*, pp. 268–275.
- Geoffrion, A.M., 2010. Lagrangian relaxation for integer programming, in: et al., M.J. (Ed.), 50 Years of Integer Programming 1958-2008. Springer. chapter 9, pp. 243–281.

- Gilmore, P., Gomory, R.E., 1965. Multistage cutting stock problems of two and more dimensions. *Operations research* 13, 94–120.
- Gilmore, P.C., Gomory, R.E., 1961. A linear programming approach to the cutting-stock problem. *Operations research* 9, 849–859.
- Heismann, O., Borndörfer, R., 2014. A generalization of odd set inequalities for the set packing problem, in: *Operations Research Proceedings 2013*. Springer, pp. 193–199.
- Hilsenbeck, O., Schwarzfischer, M., Loeffler, D., Dimopoulos, S., Hastreiter, S., Marr, C., Theis, F., Schroeder, T., 2017. fastER : a user-friendly tool for ultrafast and robust cell segmentation in large-scale microscopy. *Bioinformatics* 33, 2020–2028.
- Irnich, S., Desaulniers, G., 2005. Shortest path problems with resource constraints. *Column Generation* , 33–65.
- Kallehauge, B., Larsen, J., Madsen, O.B., Solomon, M.M., 2005. Vehicle routing problem with time windows. *Column Generation* , 67–98.
- Karp, R.M., 1972. Reducibility among combinatorial problems, in: *Complexity of computer computations*. Springer, pp. 85–103.
- Kvarnström, M., Logg, K., Diez, A., Bodvard, K., Kall, M., 2008. Image analysis algorithms for cell contour recognition in budding yeast. *Optics Express* 16, 1035–1042.
- Land, A.H., Doig, A.G., 1960. An automatic method of solving discrete programming problems. *Econometrica: Journal of the Econometric Society* , 497–520.
- Lavoie, S., Minoux, M., Odier, E., 1988. A new approach for crew pairing problems by column generation with an application to air transportation. *European Journal of Operational Research* 35, 45–58.

- Levinshtein, A., Stere, A., Kutulakos, K.N., Fleet, D.J., Dickinson, S.J., Sidiqi, K., 2009. Turbopixels: Fast superpixels using geometric flows. *IEEE Transactions on Pattern Analysis and Machine Intelligence* 31, 2290–2297.
- Liu, F., Xing, F., Yang, L., 2014. Robust muscle cell segmentation using region selection with dynamic programming, in: *IEEE International Symposium on Biomedical Imaging (ISBI)*, pp. 1381–1384.
- Mayer, C., Dimopoulos, S., Rudolf, F., Stelling, J., 2013. Using CellX to Quantify Intracellular Events. *Current Protocols in Molecular Biology* , 14.22.1–14.22.20.
- Meijering, E., 2012. Cell segmentation: 50 years down the road. *IEEE Signal Processing Magazine* , 140–145.
- Meijering, E., Carpenter, A., Peng, H., Hamprecht, F., Olivo-Marin, J.C., 2016. Imagining the future of bioimage analysis. *Nature Biotechnology* 34, 1250–1255.
- Peng, J.Y., Chen, Y.J., Green, M.D., Sabatinos, S.A., Forsburg, S.L., Hsu, C.N., 2013. PombeX: Robust cell segmentation for fission yeast transillumination images. *PLoS One* 8, e81434.
- Ronneberger, O., Fischer, P., Brox, T., 2015. U-Net: convolutional networks for biomedical image segmentation, in: Frangi, A., et al. (Eds.), *International Conference on Medical Image Computing and Computer Assisted Intervention (MICCAI)*. Springer. volume 9351 of *Lecture Notes in Computer Science*, pp. 234–241.
- Ropke, S., Cordeau, J.F., 2009. Branch and cut and price for the pickup and delivery problem with time windows. *Transportation Science* 43, 267–286.
- Rother, C., Kolmogorov, V., Lempitsky, V., Szummer, M., 2007. Optimizing binary mrfs via extended roof duality, in: *2007 IEEE Conference on Computer Vision and Pattern Recognition (CVPR)*.

- Shih, W.K., Wu, S., Kuo, Y., 1990. Unifying maximum cut and minimum cut of a planar graph. *IEEE Transactions on Computers* 39, 694–697.
- Sommer, C., Straehle, C., Koethe, U., Hamprecht, F.A., 2011. ilastik: Interactive Learning and Segmentation Toolkit, in: *IEEE International Symposium on Biomedical Imaging (ISBI)*.
- Vance, P.H., 1998. Branch-and-price algorithms for the one-dimensional cutting stock problem. *Computational Optimization and Applications* 9, 211–228.
- Vance, P.H., Barnhart, C., Johnson, E.L., Nemhauser, G.L., 1997. Airline crew scheduling: A new formulation and decomposition algorithm. *Operations Research* 45, 188–200.
- Wang, S., Wolf, S., Fowlkes, C., Yarkony, J., 2017a. Tracking objects with higher order interactions using delayed column generation, in: *International Conference on Artificial Intelligence and Statistics (AISTATS)*.
- Wang, S., Zhang, C., Gonzalez-Ballester, M.A., Ihler, A., Yarkony, J., 2017b. Multi-person pose estimation via column generation. *arXiv preprint arXiv:1709.05982*.
- Xing, F., Yang, L., 2016. Robust nucleus/cell detection and segmentation in digital pathology and microscopy images: A comprehensive review. *IEEE Reviews in Biomedical Engineering* 9, 234–263.
- Yarkony, J., 2015. Next generation multicuts for semi-planar graphs. *arXiv preprint arXiv:1511.01994*.
- Yarkony, J., Fowlkes, C., 2015. Planar ultrametrics for image segmentation, in: *Neural Information Processing Systems*.
- Yarkony, J., Ihler, A., Fowlkes, C., 2012. Fast planar correlation clustering for image segmentation, in: *Proceedings of the 12th European Conference on Computer Vision (ECCV)*.

- Yarkony, J., Zhang, C., Fowlkes, C., 2015. Hierarchical planar correlation clustering for cell segmentation, in: *Energy Minimization Methods in Computer Vision and Pattern Recognition (EMMCVPR)*, pp. 492–504.
- Zhang, C., Huber, F., Knop, M., Hamprecht, F., 2014a. Yeast cell detection and segmentation in bright field microscopy, in: *IEEE International Symposium on Biomedical Imaging (ISBI)*.
- Zhang, C., Yarkony, J., Hamprecht, F., 2014b. Cell detection and segmentation using correlation clustering, in: *International Conference on Medical Image Computing and Computer Assisted Intervention (MICCAI)*. volume 8673 of *Lecture Notes in Computer Science*, pp. 9–16.
- Zhang, Z., Schwing, A., Fidler, S., Urtasun, R., 2015. Monocular object instance segmentation and depth ordering with CNNs, in: *International Conference on Computer Vision (ICCV)*.